Colloidal CuInSe2 nanocrystals thin films of low surface roughness

Antoine De Kergommeaux, Angela Fiore, Jérôme Faure-Vincent, Adam Pron, Peter Reiss

Advances in Natural Sciences:
Nanoscience and Nanotechnology

Colloidal $CuInSe_2$ nanocrystals thin films of low surface roughness*

OPEN ACCESS
IOP PUBLISHING
ADVANCES IN NATURAL SCIENCES: NANOSCIENCE AND NANOTECHNOLOGY
Adv. Nat. Sci.: Nanosci. Nanotechnol. **4** (2013) 015004 (6pp)
doi:10.1088/2043-6262/4/1/015004

Colloidal $CuInSe_2$ nanocrystals thin films of low surface roughness*

Antoine de Kergommeaux[1], Angela Fiore[1], Jérôme Faure-Vincent[1], Adam Pron[1,2] and Peter Reiss[1]

[1] Laboratoire d'Electronique Moléculaire, Organique et Hybride, SPrAM, UMR 5819 CEA/CNRS/UJF-Grenoble 1, INAC, 17 rue des Martyrs, F-38054 Grenoble, France
[2] Faculty of Chemistry, Warsaw University of Technology, Noakowskiego 3, Poland

E-mail: peter.reiss@cea.fr

Received 29 October 2012
Accepted for publication 30 December 2012
Published 29 January 2013
Online at stacks.iop.org/ANSN/4/015004

Abstract
Thin-film processing of colloidal semiconductor nanocrystals (NCs) is a prerequisite for their use in (opto-)electronic devices. The commonly used spin-coating is highly materials consuming as the overwhelming amount of deposited matter is ejected from the substrate during the spinning process. Also, the well-known dip-coating and drop-casting procedures present disadvantages in terms of the surface roughness and control of the film thickness. We show that the doctor blade technique is an efficient method for preparing nanocrystal films of controlled thickness and low surface roughness. In particular, by optimizing the deposition conditions, smooth and pinhole-free films of 11 nm $CuInSe_2$ NCs have been obtained exhibiting a surface roughness of 13 nm root mean square (rms) for a 350 nm thick film, and less than 4 nm rms for a 75 nm thick film.

Keywords: semiconductor nanocrystals, $CuInSe_2$, thin film deposition, solar cells

Classification numbers: 4.03, 5.01, 2.03, 5.03, 6.03

1. Introduction

Colloidal semiconductor nanocrystals (NCs) are promising materials for use as light absorbers or sensitizers in optoelectronic devices such as, for example, photovoltaic cells or photodiodes [1–13]. They offer the possibility of low-cost solution processing and benefit from size-tunable properties due to quantum confinement effects, which facilitate the adjustment of their electronic energy levels and absorption spectrum [14–16]. $CuInSe_2$ is a well-known material in thin-film solar cell technology where the control of the band gap is achieved by the addition of gallium resulting in Cu(In, Ga)Se_2 (CIGS) [17]. However, the precise control of the composition and crystallographic phase of the quaternary material is technologically challenging throughout the different preparation and processing steps. In the form of colloidal NCs, on the other hand, the band gap of $CuInSe_2$ can be conveniently varied from the bulk value of 1.0 eV to 1.5 eV when the crystal size is reduced from 20 nm to around 3 nm in diameter [18]. At the same time, the shape and crystal structure of the NCs can be controlled by varying the reaction parameters during chemical synthesis. The obtained NC 'inks' can be deposited on substrates using various wet techniques such as drop-casting, spin-, dip-, or spray-coating, each of them presenting advantages and drawbacks. In particular, the preparation of dense NC films showing no pinholes, low surface roughness and a thickness of several hundreds of nanometres is still a delicate matter. Films with the aforementioned characteristics are of particular interest for the fabrication of NC based solar cells. Recently doctor blading, a technique derived from screen-printing, emerged as a promising alternative to the cited NC deposition methods [19–22]. With this technique, films of hundreds of nanometres thickness can be achieved in one run by the simple spreading of the NC ink with a blade. Another appealing feature is the low materials consumption as compared to techniques like spin-coating. Herein, we study the influence of several experimental parameters, namely the concentration of the NC colloidal solution, the solvent and the substrate type, on the properties of thin films of $CuInSe_2$ NCs prepared by the doctor blade technique.

* Invited talk at the 6th International Workshop on Advanced Materials Science and Nanotechnology, 30 October–2 November 2012, Ha Long, Vietnam.

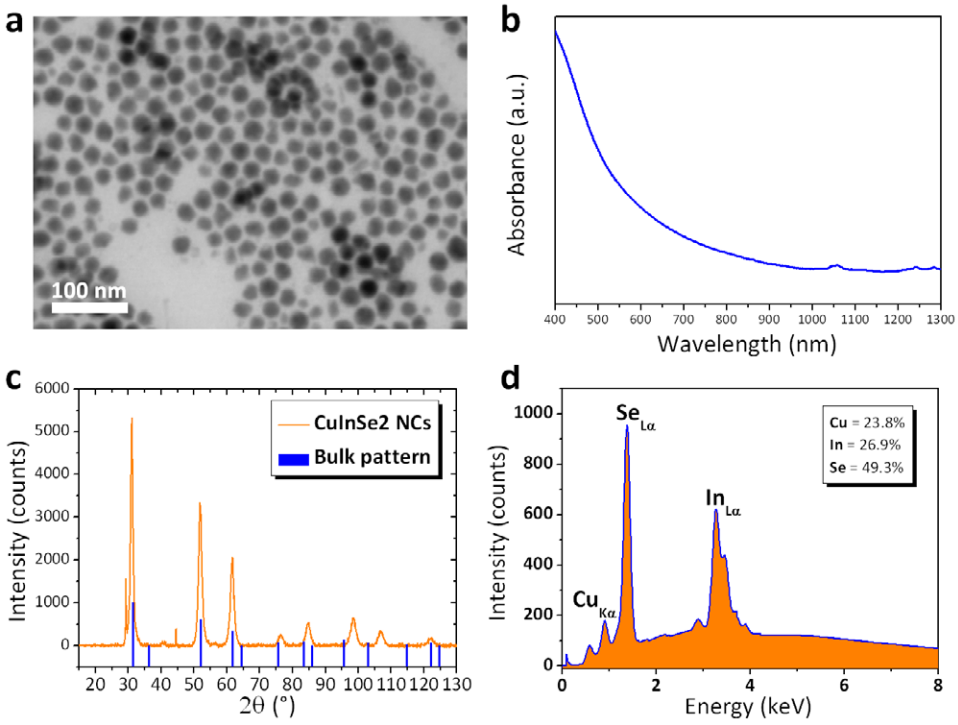

Figure 1. (a) STEM image of the as-synthesized $CuInSe_2$ NCs; (b) UV–Vis–NIR absorption spectrum; (c) powder x-ray diffractogram (Co-Kα) compared to the pattern of bulk cubic $CuInSe_2$ in the space group F-43m (JCPDS #01–075-2919); and (d) EDS spectrum of the NCs deposited on a silicon substrate.

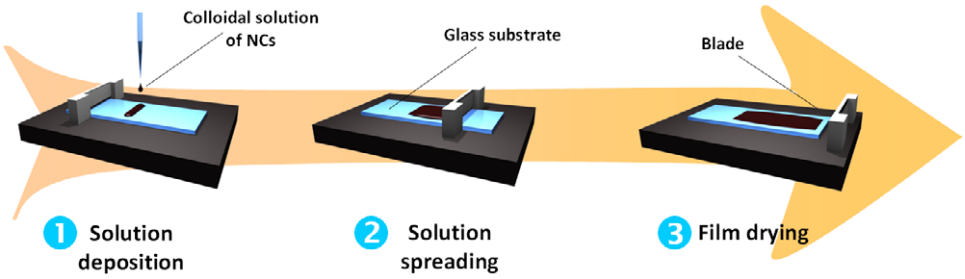

Figure 2. Scheme describing the doctor blade deposition method. First step: the colloidal solution is deposited onto glass substrate, second step: the blade spreads the solution over the substrate; third step: the obtained film is dried.

2. Experimental

2.1. Synthesis of $CuInSe_2$ NCs

We synthesized $CuInSe_2$ NCs following the protocol developed in our previous work [13]. It is based on the reaction between copper and indium chloride and selenourea. Briefly, in a 50 ml flask, 0.05 g of CuCl (0.5 mmol), 0.11 g of $InCl_3$ (0.5 mmol) and 10 ml of oleylamine are vigorously stirred and degassed for 1 h at 60 °C under primary vacuum using a Schlenk line. The temperature of the mixture is then increased to 130 °C under argon flow, during which the colour of the solution changes from blue to yellow. In a second flask, 0.123 g of selenourea (1.0 mmol) is dissolved in 1 ml of oleylamine by heating to 200 °C under argon flow. The first flask is then cooled to 100 °C. The selenium precursor from the second flask is quickly injected into the first one and the temperature is immediately increased to 240 °C. After 1 h at this temperature, the solution is cooled to room temperature and 30 ml of ethanol are added to precipitate the NCs. Centrifugation at 7000 rpm for 3 min is used to isolate the NCs, which are redissolved in chloroform. To remove incompletely stabilized NCs, the obtained dispersion is centrifuged again at 7000 rpm for 5 min.

2.2. Preparation of thin films of $CuInSe_2$ NCs

For thin-film deposition we use an Erichsen Doctor Blade system operated under air with a blade distance from the substrate of 50 μm. Colloidal solutions of $CuInSe_2$ NCs are prepared at different concentrations (cf text) in toluene or 1,2-dichlorobenzene (DCB). The substrates (26 × 75 mm glass slides or 17 × 25 mm ITO-coated glass substrates) are cleaned prior to use by immersion in an ultrasonic bath with acetone for 10 min followed by ethanol for a further 10 min. Just before the deposition, the substrates are put into a UV/ozone cleaner for 10 min. An amount of 7–20 μl of the NCs colloidal solution is deposited on one end of the substrate and the blade is moved with a speed of 2.5 mm s^{-1} while applying a temperature of 110 °C in the case of toluene and 150 °C in the case of DCB to the table. After blading,

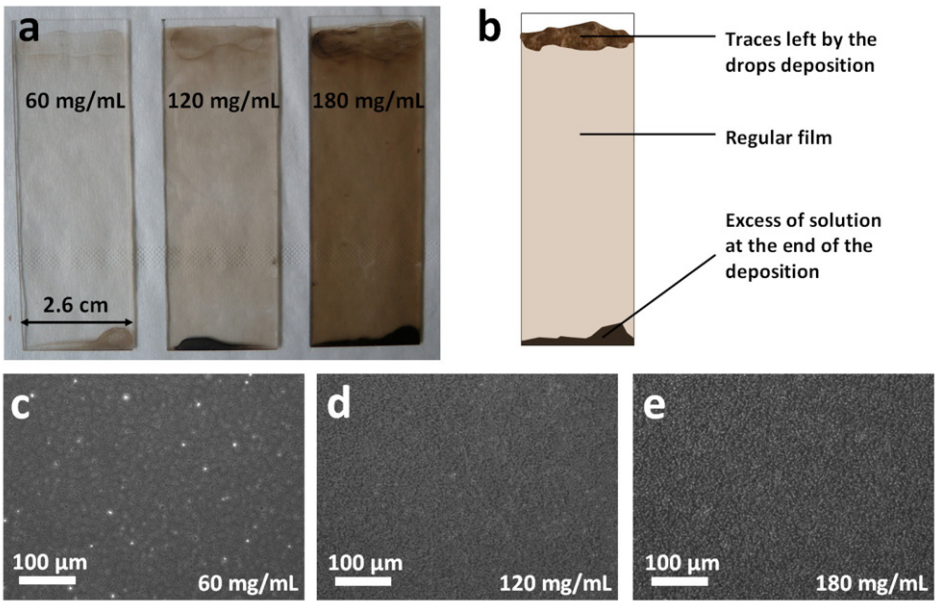

Figure 3. (a) Photographs of films deposited on glass substrates using NC concentrations of 60, 120 and 180 mg ml^{-1} (from left to right); (b) scheme of the as-deposited film and the left-traces; and (c)–(e) optical microscopy images of the three films in transmission mode.

the film is left drying for 5 min. No further thermal treatment is employed.

2.3. Characterization techniques

The obtained NCs and thin films are analysed using a ZEISS Ultra 55+ scanning electron microscope (SEM) and a NANOSURF atomic force microscope (AFM). For the determination of the NCs' size and size distribution, they are drop-cast on a carbon-coated copper grid (Ted-Pella) and the SEM is used in scanning transmission electronic microscopy (STEM) mode. Powder x-ray diffraction is carried out using a PHILIPS X'Pert powder diffractometer (Co-Kα $\lambda =$ 1.789 Å). Ultraviolet–visible–near infrared (UV–Vis–NIR) absorption spectra were measured with a Perkin-Elmer Lambda 900 spectrometer (wavelength range 200–3300 nm).

3. Results and Discussion

3.1. Characterization of the $CuInSe_2$ NCs

Figure 1(a) shows a STEM image of the obtained $CuInSe_2$ NCs presenting an average size of 11 nm. The UV–Vis–NIR absorption spectrum (figure 1(b)) shows a threshold at around 900 nm and by plotting the square of absorbance versus energy, a direct band gap of 1.4 eV can be extracted. For 11 nm diameter NCs the widening of the band gap with respect to the bulk material (1.0 eV) is expected due to quantum confinement, the Bohr exciton radius being estimated as 10.6 nm [23]. The powder x-ray diffractogram of the NCs (figure 1(c)) shows the cubic phase in the space group F-43m ($a = b = c = 5.798$ Å) as observed on macroscopic powders [24]. The Scherrer formula applied on the peaks (111), (220) and (311) gives an average crystallite size of 10 nm, coherent with the STEM observations. The two narrow peaks at 29° and 45° could be attributed by further analysis to the used surfactants. Finally, energy-dispersive x-ray spectroscopy (EDS) analysis (figure 1(d)) confirms that the stoichiometry of the $CuInSe_2$ NCs is close to 1 : 1 : 2 (Cu = 24%, In = 27%, and Se = 49%). In bulk $CuInSe_2$ copper vacancies in the crystal lattice have been shown to enhance conductivity [25].

3.2. Thin-film preparation and macroscopic analysis

The doctor blade deposition technique, schematically illustrated in figure 2, finds broad application in ceramics where a paste containing the ceramic powder together with a solvent, a binder and a plasticizer is spread onto a substrate by a blade. A post-deposition treatment can be applied in order to improve the surface quality through pressing, laminating or shaping. Finally, a thermal treatment is generally applied in order to burn the organic compounds (binder and plasticizer), eventually followed by a sintering step. Bodnarchuk *et al* adapted the doctor blade technique for the deposition of colloidal bimetallic nanoparticles and prepared perfectly ordered monolayers of comparably large lateral dimensions [20]. Here we focus on the preparation of thicker films, in a range from tens to hundreds of nanometres, which are of particular interest for optoelectronic applications.

As the doctor blade technique avoids material losses, the amount of colloidal solution used for covering approximately 10 cm^2 is only 20 μl. First we study the influence of the concentration of the NCs' colloidal solution on the film thickness and surface roughness. The photographs presented in figure 3(a) show at first glance that the film thickness is proportional to the concentration. At the beginning and the end of the film, some traces are visible, enhanced in the scheme, figure 3(b). The former arise from partial evaporation occurring between the moments of ink drop deposition and spreading with the blade; the latter can be explained by the excess ink left at the end of the process. However, in between these traces, the film is visually homogeneous in colour and aspect. Optical microscope images shown in figures 3(c)–(e) confirm the uniformity of the films on the macroscopic scale.

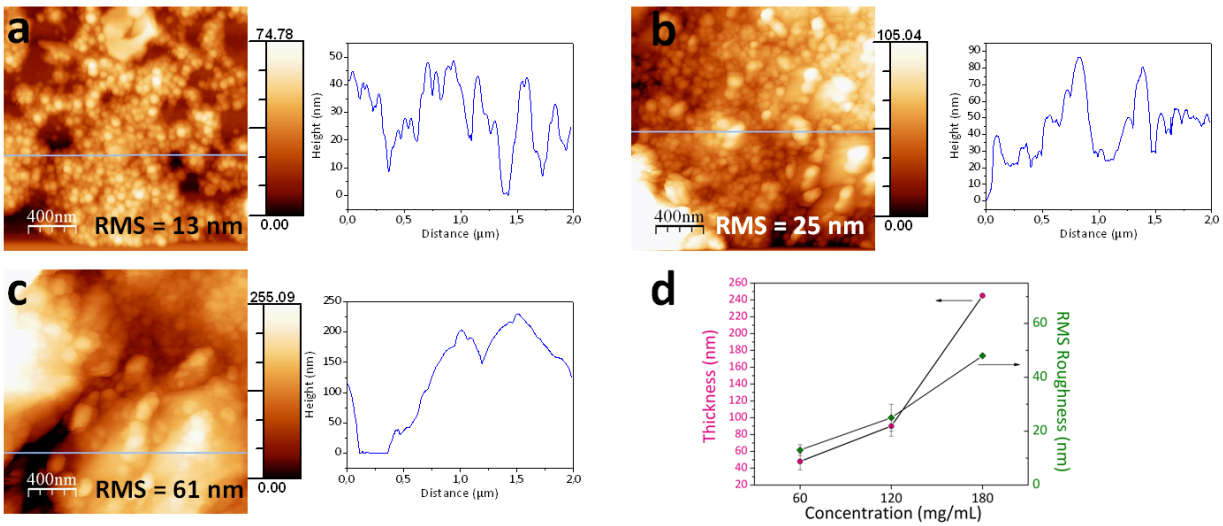

Figure 4. (a)–(c) AFM topographic images of films deposited from toluene using an NC concentration of 60, 120 and 180 mg ml^{-1}, respectively (110 °C, image area $2 \times 2\,\mu m^2$). The corresponding height profiles along the lines are shown next to each image. (d) Evolution of the film thickness and surface roughness as a function of the concentration of the NC colloidal solution.

The image corresponding to the concentration of 60 mg ml^{-1} exhibits some pinholes visible as white spots generated by the transmission mode used for the analysis.

3.3. Analysis of the surface roughness of as-deposited films

In addition to the surface state of the NCs, their arrangement and interparticle distance strongly impact the electrical conduction properties of the obtained films. AFM imaging combined with the analysis of surface roughness allows for the morphological characterization of the films on the nanoscale. As seen in figure 4, AFM images reveal the formation of NC assemblies or aggregates whose dimensions depend on the used ink concentration. The root mean square (rms) roughness of the films is increasing with ink concentration from 13 nm for 60 mg ml^{-1} to 61 nm for 180 mg ml^{-1}. This significant increase of inhomogeneity appears even more pronounced when analysing the corresponding height profiles revealing peak-to-peak distances rising from 40 to 230 nm when using concentrations of 60 and 180 mg ml^{-1}, respectively. For such elevated surface roughness values, the film thickness is difficult to evaluate with standard profilometer measurements. However, AFM analysis enables us to determine an average film thickness of 35, 63 and 188 nm for the films deposited with an ink concentration of 60, 120 and 180 mg ml^{-1}, respectively.

Figure 4(d) summarizes the evolution of the film thickness and rms roughness as a function of the concentration of the colloidal solution. While the correlation between thickness and concentration is expected, the strong increase of the surface roughness when using more concentrated inks while keeping all other deposition parameters constant suggests possible aggregation phenomena prior to the spreading.

In order to prepare thicker films without increasing surface roughness, we replace toluene by the higher boiling point solvent 1,2-dichlorobenzene (boiling point 180 °C instead of 111 °C). Slower solvent evaporation generally allows for the better organization and packing of NCs, leading to smoother films even at high concentration. Using a colloidal solution of 180 mg ml^{-1} and a table temperature of 150 °C instead of 110 °C, we perform film deposition under otherwise identical conditions. The as-deposited film analysed by AFM (figure 5) exhibits a significantly lower roughness of 13 nm rms as compared to the film deposited from toluene using the same concentration (61 nm), while obtaining a film thickness of around 350 nm.

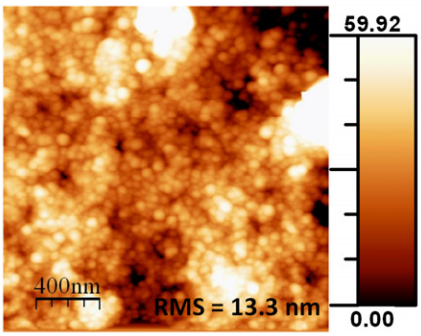

Figure 5. AFM topographic image of NCs film deposited from 1,2-dichlorobenzene (180 mg ml^{-1}, 150 °C). The image size is $2 \times 2\,\mu m^2$.

3.4. Deposition on indium tin oxide (ITO)-coated substrates

Finally, film deposition is carried out on ITO-coated glass substrates, widely used as transparent electrodes. UV/ozone treatment of the substrates is performed right before deposition in order to remove organic contamination and to increase the ITO surface energy favouring NC adhesion. We deposit 7 μl of a 100 mg ml^{-1} colloidal solution in toluene using a table temperature of 80 °C and the (standard) deposition speed of 2.5 mm s^{-1}. As seen in figure 6, the obtained film is dense and homogeneous. In particular, the SEM images (figures 6(a) and (c)) reveal the absence of

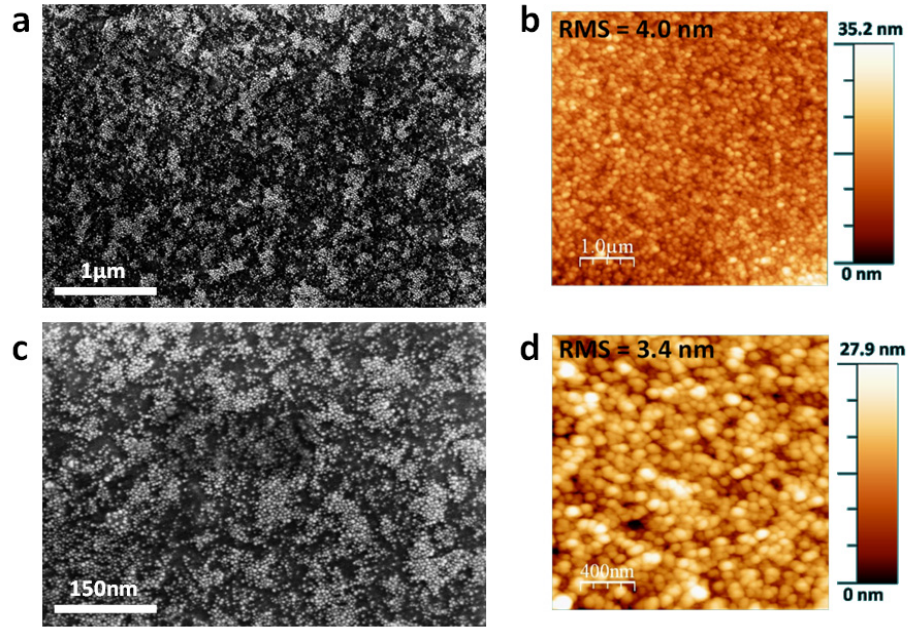

Figure 6. (a), (c) Top view SEM images of a $CuInSe_2$ NCs film on an ITO-coated glass substrate at different magnifications; (b), (d) AFM topographic images of the same film (b) $5 \times 5\ \mu m^2$; (d) $2 \times 2\ \mu m^2$ area.

pinholes, while AFM measurements show a very low surface roughness value of 4.0 nm rms for $5 \times 5\ \mu m^2$ and 3.4 nm rms for $2 \times 2\ \mu m^2$ surface area and a film thickness of 76 nm. We attribute the strongly reduced surface roughness as compared to the deposition on glass substrates under similar conditions (cf figure 4(b)) to the different wetting behaviour of the NCs on ITO.

3.5. Solar cell characterization

Schottky-type solar cells have been realized as described in [13] by evaporation of Al/Au top contacts on $CuInSe_2$ NCs films deposited on ITO-coated glass substrates. I/V measurements (not shown) reveal the absence of diode characteristics and no photovoltaic effect is observed under irradiation with simulated solar light. We attribute this behaviour to the low conductivity within the NC thin films originating from the highly insulating character of the oleylamine surface ligands [26]. Similar studies comprising surface ligand exchange with smaller molecules prior to doctor blade deposition are currently underway.

4. Conclusion

We show that doctor blade coating is an appropriate tool for deposition of colloidal NCs inks as films of controlled thickness on various flat substrates. The low materials consumption makes this technique compatible with cost-efficient thin-film processing on large surfaces. The film thickness can be conveniently controlled by adjusting the concentration of the NCs' colloidal solution, while surface roughness depends on the solvent evaporation conditions and on the nature and pretreatment of the substrate surface. Using optimized deposition parameters, dense and smooth NC films without pinholes can be obtained in a thickness range of several tens to several hundreds of nanometres, which are suitable for use in (opto–)electronic applications.

Acknowledgment

This research was supported by the Micro-Nano and Energy research clusters of the region Rhônes-Alpes.

References

[1] Mitzi D B, Copel M and Chey S J 2005 *Adv. Mater.* **17** 1285–9
[2] Talapin D V and Murray C B 2005 *Science* **310** 86–9
[3] Shimoda T, Matsuki Y, Furusawa M, Aoki T, Yudasaka I, Tanaka H, Iwasawa H, Wang D, Miyasaka M and Takeuchi Y 2006 *Nature* **440** 783–6
[4] Ong B S, Li C, Li Y, Wu Y and Loutfy R 2007 *J. Am. Chem. Soc.* **129** 2750–1
[5] Urban J J, Talapin D V, Shevchenko E V, Kagan C R and Murray C B 2007 *Nature Mater.* **6** 115–21
[6] Luther J M, Law M, Beard M C, Song Q, Reese M O, Ellingson R J and Nozik A J 2008 *Nano Lett.* **8** 3488–92
[7] Panthani M G, Akhavan V, Goodfellow B, Schmidtke J P, Dunn L, Dodabalapur A, Barbara P F and Korgel B A 2008 *J. Am. Chem. Soc.* **130** 16770–7
[8] Fiore A *et al* 2009 *J. Am. Chem. Soc.* **131** 2274–82
[9] Tang J *et al* 2011 *Nature Mater.* **10** 765–71
[10] Gao J, Luther J M, Semonin O E, Ellingson R J, Nozik A J and Beard M C 2011 *Nano Lett.* **11** 1002–8
[11] Talapin D V, Lee J-S, Kovalenko M V and Shevchenko E V 2010 *Chem. Rev.* 389–458
[12] Lee J S, Kovalenko M V, Huang J, Chung D S and Talapin D V 2011 *Nature Nanotechnol.* **6** 348–52
[13] de Kergommeaux A, Fiore A, Bruyant N, Chandezon F, Reiss P, Pron A, de Bettignies R and Faure-Vincent J 2011 *Sol. Energy Mater. Sol. Cells* **95** S39–43
[14] Brus L E 1984 *J. Chem. Phys.* **80** 4403–9
[15] Brus L E 1986 *J. Phys. Chem.* **90** 2555–60
[16] Hines M A and Scholes G D 2003 *Adv. Mater.* **15** 1844–9
[17] Siebentritt S, Igalson M, Persson C and Lany S 2010 *Prog. Photovolt.* **18** 390–410
[18] Cassette E, Pons T, Bouet C, Helle M, Bezdetnaya L, Marchal F and Dubertret B 2010 *Chem. Mater.* **22** 6117–24

[19] Hotza D and Greil P 1995 *Mater. Sci. Eng.* A **202** 206–17
[20] Kaelin M, Rudmann D and Tiwari A N 2004 *Sol. Energy* **77** 749–56
[21] Kaelin M, Rudmann D, Kurdesau F, Zogg H, Meyer T and Tiwari A N 2005 *Thin Solid Films* **480–481** 486–90
[22] Bodnarchuk M I, Kovalenko M V, Pichler S, Fritz-Popovski G, Hesser G and Heiss W 2010 *ACS Nano* **4** 423–31
[23] Castro S L, Bailey S G, Raffaelle R P, Banger K K and Hepp A F 2003 *Chem. Mater.* **15** 3142–7
[24] Merino J M, Di Michiel M and León M 2003 *J. Phys. Chem. Sol.* **64** 1649–52
[25] Naghavi N *et al* 2010 *Prog. Photovolt.* **18** 411–33
[26] de Kergommeaux A, Fiore A, Faure-Vincent J, Chandezon F, Pron A, de Bettignies R and Reiss P 2012 *Mater. Chem. Phys.* **136** 877–82